Synthesis and Characterization of Poly(ethylene glycol)-*b*-Poly(ε-caprolactone) Copolymers with Functional Side Groups on the Polyester Block

Wen-Hsin Chen,[1] Mu-Yi Hua,[1] Ren-Shen Lee[2]

[1]*Department of Chemical and Materials Engineering, Chang Gung University, Tao-Yuan, Taiwan, Republic of China*
[2]*Center of General Education, Chang Gung University, Kwei-Shan, Tao-Yuan 333, Taiwan, Republic of China*

Received 26 May 2011; accepted 7 October 2011
DOI 10.1002/app.36225
Published online 31 January 2012 in Wiley Online Library (wileyonlinelibrary.com).

ABSTRACT: This study reports the successful synthesis of amphiphilic MPEG-*b*-PCL based-block copolymers bearing benzyloxy and hydroxyl side groups on the PCL block by ring-opening polymerization of 4-benzyloxy-ε-caprolactone (4-BOCL) and ε-caprolactone (ε-CL) with methoxy PEG (550 g mol^{-1}) as the initiator and Tin(II) 2-ethylhexanoate ($SnOct_2$) as the catalyst. These copolymers were characterized by differential scanning calorimetry (DSC), ^1H NMR, and gel permeation chromatography. The thermal properties (T_g and T_ms) of the block copolymers depend on the polymer composition. Incorporating a greater amount of 4-BOCL and/or ε-CL was incorporated into the macromolecular backbone causes a decrease T_g, and an increase in T_ms. The micellar characteristics in the aqueous phase were investigated by fluorescence spectroscopy, transmission electron microscopy (TEM), and dynamic light scattering (DLS). A lower critical micelle concentration (CMC) was observed in $MPEG_{12}$-*b*-$PBOCL_{12}$-*b*-PCL series, which have higher hydrophobic components in the copolymers. However, contrasting results were observed for $MPEG_{12}$-*b*-$PBOCL_{27}$-*b*-PCL systems. The micelle exhibited a spindle shape, with an average size of less than 200 nm. A weak drug entrapment efficiency and drug-loading ability of these micelles were observed. © 2012 Wiley Periodicals, Inc. J Appl Polym Sci 125: 2902–2913, 2012

Key words: amphiphilic; functional MPEG-*b*-PCL based-block copolymer; 4-benzyloxy-ε-caprolactone; micelle

INTRODUCTION

Amphiphilic copolymers are well known for self-assembly into micelles or larger aggregates in selective solvents for one block. In aqueous solution, they commonly form a core-shell structure with a hydrophobic core surrounded by a hydrated hydrophilic shell. The properties of block copolymer micelles in biomedical applications, namely the efficacious delivery of hydrophobic drugs sequestered within micellar cores, have been studied extensively.[1–7]

Introducing functional groups to the polyester segment of PEG-*b*-polyester block copolymers such as PEG-*b*-poly(ε-caprolactone) (PEG-*b*-PCL) may result in the development of biodegradable self-assembling biomaterials with a potential for attaching different reactive compounds to the core-forming structure.[8–13] On the other hand, the attachment of reactive groups to the core-forming segment of the PEG-*b*-PCL block copolymers provides additional opportunities to modify the thermodynamic and kinetic stability, biodegradation, drug solubility, and release properties of PEG-*b*-PCL micelles.[14–23] Recently, PEO-*b*-PCL block copolymers with benzyl carboxylate or carboxylic groups have been prepared by the ring-opening polymerization of 4-benzyl carboxylate-ε-caprolactone (4-BCCL) using PEO as the macroinitiator.[24] PEO-*b*-PBCL and PEO-*b*-PCCL block copolymers assembled to spherical micelles having average diameters of 62 and 20 nm. Biodegradable PEO-*b*-poly(ester) micelles with benzyl carboxylate and carboxyl groups in the micellar core have tremendous potential in the design of optimized carriers for the delivery of various therapeutic agents.

Previous research,[25] reports the synthesis and micellar characterization of amphiphilic block copolymers based on hydrophilic poly(ethylene glycol) methyl ether macroinitiators and hydrophobic poly(4-methyl-ε-caprolactone) (PMCL) or poly(4-phenyl-ε-caprolactone) (PBCL). This article reports the successful synthesis and self-assembly of MPEG-*b*-PCL based-block copolymers bearing benzyloxy and hydroxyl functional groups, i.e., MPEG-*b*-poly

Correspondence to: R.-S. Lee (shen21@mail.cgu.edu.tw).
Contract grant sponsor: National Science Council; contract grant number: NSC 96-2221-E-182-023.
Contract grant sponsor: Chang Gung University; contract grant number: BMRP 123.

(4-benzyloxy-ε-caprolactone)s (MPEG-*b*-PBOCL)s diblock copolymers, MPEG-*b*-poly(4-benzyloxy-ε- caprolactone)-*b*-poly(ε-caprolactone)s (MPEG-*b*-PBOCL-*b*-PCL)s, and debenzylation MPEG-*b*-poly(4-hydroxyl-ε-caprolactone)-*b*-poly(ε-caprolactone) (MPEG-*b*-PHOCL-*b*-PCL) triblock copolymers. The presence of benzyloxy or hydroxyl groups on the core-forming block makes it possible to modify the polymer's hydrophobicity, and crystallinity. This study investigates the micellar characteristics of these functional MPEG-*b*-PCL based-block copolymers in the aqueous phase with fluorescence spectroscopy, dynamic light scattering (DLS), and transmission electron microscopy (TEM).

EXPERIMENTAL

Materials

MPEG 550 g mol^{-1} ($MPEG_{12}$, DP = 12), 1,4-cyclohexanediol, benzyl bromide, palladium-on-charcoal (10 wt %), pyrene, amitriptyline hydrochloride (AM) were obtained from Aldrich Chemical Co. *m*-Chloroperoxybenzoic acid (*m*-CPBA) was purchased from Fluka Chemical Co. Tin(II) 2-ethylhexanoate ($SnOct_2$) was obtained from Strem and used as received. ε-CL (Aldrich) was dried and vacuum-distilled over calcium hydride. Organic solvents such as tetrahydrofuran (THF), methanol, chloroform, and *n*-hexane of high pressure liquid chromatography (HPLC) grade were used without further purification. Ultrapure water purified with a Milli-Q Plus (Waters) was used.

Preparation of 4-benzyloxy-ε-caprolactone

The preparation of 4-benzyloxy-ε-caprolactone was according to the reported method from 1,4-dihydroxycyclohexane.[26] The overall yield was 20.1%. ^{1}H NMR ($CDCl_3$) δ1.82–2.09 (m, 4H,—CH_2CH(OBz)CH_2—), 2.41–2.48 (ddd, 1H, —CH_2CO_2—), 2.98–3.10 (ddd, 1H, —CH_2CO_2—), 3.79–3.83 (m, 1H, —C*H*(OBz)—), 4.08 (ddd, 1H, —CO_2CH_2—), 4.57 (s, 2H, —OCH_2Ph—), 4.66 (m, 1H, —CO_2CH_2—), 7.31–7.39 (m, 5H, —Ph).

Synthesis of hydroxyl-terminated $MPEG_{12}$-*b*-PBOCL diblock copolymer

All glassware was oven dried and handled under a dry nitrogen stream. The typical polymerization process to produce $MPEG_{12}$-*b*-$PBOCL_{27}$ is as follows. $MPEG_{12}$ (M_n = 550 g mol^{-1}) (0.32 g, 0.57 mmol) and 4-BOCL (3.76 g, 17.1 mmol) were introduced into a flask and heated under a dry nitrogen stream to dissolve the 4-BOCL. Then, 61.2 mg (1.5 wt %) of $SnOct_2$ was added to the flask. The flask was purged with nitrogen and reacted at 140°C for 48 h. The resulting product was dissolved in $CHCl_3$, and then precipitated into excess *n*-hexane with stirring. The purified polymer was dried *in vacuo* at 50°C for 24 h and then analyzed. Figure 1(A) shows the ^{1}H NMR spectrum of the $MPEG_{12}$-*b*-$PBOCL_{27}$.

Synthesis of $MPEG_{12}$-*b*-PBOCL-*b*-PCL triblock copolymers

$MPEG_{12}$-*b*-$PBOCL_{27}$ with hydroxyl end groups obtained above, various molar ratios of ε-CL, and a dry stirring bar were placed in a two-neck round-bottomed flask. The polymerization was reacted at 110°C in the presence of a $SnOct_2$ (1.5 wt % based on the weight of $MPEG_{12}$-*b*-$PBOCL_{27}$ and ε-CL) catalyst under a dry nitrogen stream for 24 h. The resulting product was dissolved in $CHCl_3$, and then precipitated into excess *n*-hexane with stirring. The purified polymer was dried *in vacuo* at 50°C for 24 h and then analyzed. Figures 1(B) and 2(A) show the ^{1}H NMR and IR spectra of the $MPEG_{12}$-*b*-$PBOCL_{27}$-*b*-PCL_{48}.

Deprotection of the benzyloxy-protecting group of new copolymer

A 10 wt % palladium-on-charcoal catalyst (0.1 g) was added to a 10 mL solution of the $MPEG_{12}$-*b*-$PBOCL_{27}$-*b*-PCL_{89} (0.5 g) whose hydroxyl groups were protected by benzyl in THF/CH_3OH (v/v = 3/1). After purging with nitrogen three times, the reaction mixture was stirred under 1.0 atm hydrogen pressure at 50°C for 24 h. After this deprotection reaction, the catalyst was removed by filtration, and the solution was concentrated to approximately one-fourth its original volume under reduced pressure. The concentrated solution was poured into diethyl ether to precipitate, yielding deprotected polymer $MPEG_{12}$-*b*-$PHOCL_{22}$/$PBOCL_5$-*b*-PCL_{89} which was then analyzed by ^{1}H NMR and FT-IR. Figures 1(C) and 2(B) show the ^{1}H NMR and IR spectra of $MPEG_{12}$-*b*-$PHOCL_{22}$/$PBOCL_5$-*b*-PCL_{89}.

Characterization

^{1}H NMR spectra were obtained using a Bruker WB/DMX-500 spectrometer (Ettlingen, Germany) at 500 MHz with chloroform (δ = 7.24 ppm) as an internal standard in chloroform-*d* ($CDCl_3$). IR spectra were measured using a Bruker TENSOR 27 Fourier transform infrared (FTIR) spectrophotometer. Samples were either neatly placed on NaCl plates or pressed into KBr pellets. A DuPont 9900 system consisting of DSC (Newcastle, DE) performed a thermal analysis of the polymer. The heating rate was 20°C min^{-1}. The T_gs were read at the middle of the change in the heat capacity and were taken from the second

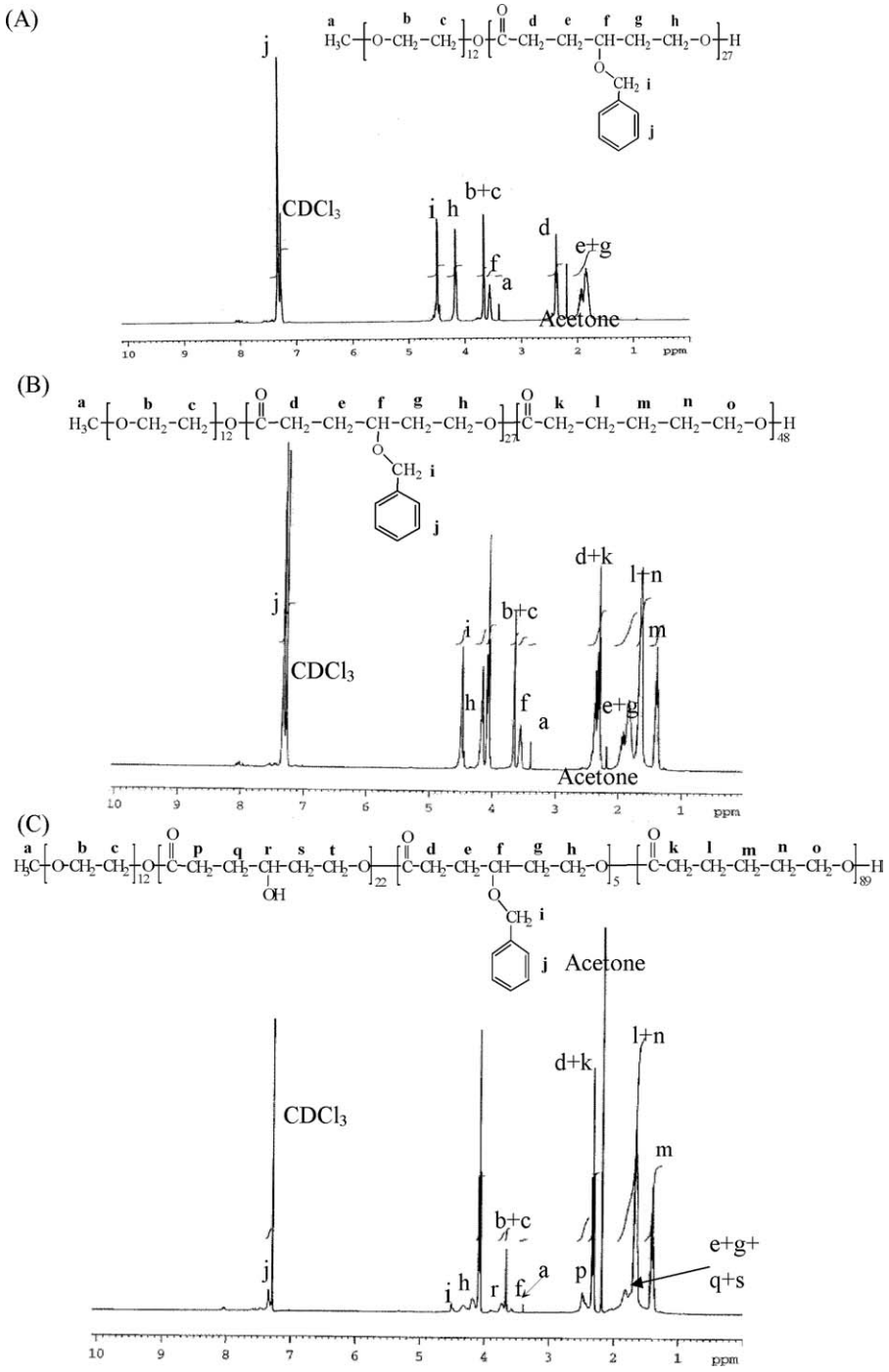

Figure 1 Representative ^{1}H NMR spectroscopy of (A) $MPEG_{12}$-*b*-$PBOCL_{27}$, (B)$MPEG_{12}$-*b*-$PBOCL_{27}$-*b*-PCL_{48}, and (C) $MPEG_{12}$-*b*-$PHOCL_{22}$/$PBOCL_5$-*b*-PCL_{89}.

heating scan after quick cooling. The number-average molecular weight (M_n) and weight-average molecular weights (M_w, respectively) of the polymer were determined with a GPC system. It was carried out on a Jasco HPLC system equipped with a model PU-2031 refractive-index detector (Tokyo, Japan), and Jordi Gel polydivinyl benzene (DVB) columns with pore sizes of 100, 500, and 10^3 Å. Chloroform was used as the eluent at a flow rate of 0.5 mL min^{-1}. Polystyrene standards with a low dispersity (Polymer Sciences) generated a calibration curve. Data were recorded and manipulated with a Windows-based software package (Scientific Information Service Co.).

Ultraviolet-visible (UV-vis) spectra were obtained with a Jasco V-550 spectrophotometer (Tokyo, Japan). The pyrene fluorescence spectra were recorded on a Hitachi F-4500 spectrofluorometer (Japan) using

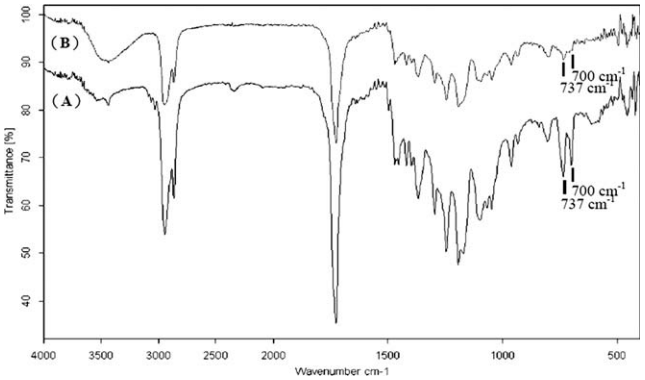

Figure 2 IR spectra of $MPEG_{12}$-*b*-$PBOCL_{27}$-*b*-PCL_{89} (A) before and (B) after deprotection.

square quartz cells (1.0 × 1.0 cm^2). For fluorescence excitation spectra, the detection wavelength λ_{em} was set at 390 nm.

Preparation of polymeric micelles

Polymeric micelles of MPEG-*b*-PBOCL-*b*-PCL copolymers were prepared using the dialysis method. Briefly, a solution of MPEG-*b*-PBOCL-*b*-PCL copolymer (30 mg) in DMF (5 mL) was placed in a dialysis bag (MWCO = 3500) and dialyzed against deionized (DI) water at ambient temperature for 24 h. The water was replaced at 2 h intervals.

Measurements of fluorescence spectroscopy

To prove micelle formation, fluorescence measurements were carried out using pyrene as a probe.[27] The fluorescence spectra of pyrene in aqueous solution were recorded at room temperature on a fluorescence spectrophotometer. The sample solutions were prepared by first adding known amounts of pyrene in acetone to a series of flasks. After the acetone had evaporated completely, measured amounts of micelle solutions with various concentrations of $MPEG_{12}$-*b*-$PBOCL_{12}$-*b*-PCL_{33} (75, 18.75, 9.38, 4.69, 0.29, and 0.018 mg L^{-1}) were added to each flasks and mixed via vortexing. The concentration of pyrene in the final solutions was 6.1 × $10^{-7}M$. The flasks were allowed to stand overnight at room temperature to equilibrate the pyrene and the micelles. The excitation spectra for pyrene had an emission wavelength of 390 nm.

Measurements of size and size distribution

The size distribution of micelles was estimated by a dynamic light scattering (DLS) using a Particle-Size Analyzer (Zetasizer nano ZS, Malvern, UK) at 20°C. The scattered light intensity was detected at 90° to an incident beam. Measurements were taken after the aqueous micellar solution ($C = 0.3$ g L^{-1}) was filtered by a microfilter with an average pore size of 0.2 μm (Advantec MFS). The average size distribution of the aqueous micellar solution was determined based on the CONTIN programs developed by Provencher and Hendrix.[28]

Observation on transmission electron microscope

The morphology of the micelles was observed by TEM (JEM 1200-EXII, Tokyo, Japan). Drops of micelle solution ($C = 0.3$ g L^{-1}) were placed on a carbon film coated on a copper grid, and then were dried at room temperature. Observations were made at an accelerating voltage of 100 kV.

Zeta potential measurement

Zeta potential was measured by a laser Doppler anemometer (Zetasizer nano ZS, Malvern, UK). Before measurement, the particle suspension was diluted with deionized water. The value was recorded as the average of five measurements.

Determination of drug-loading content and drug entrapment efficiency

Using the oil-in-water solvent evaporation method, $MPEG_{12}$-*b*-PBOCL-*b*-PCL (50-fold CMC value) was dissolved in 6 mL methylene chloride, followed by adding antitriptyline hydrochloride (AM) with various weight ratios to polymer (1/10–1/1) as a model drug. The solution was added dropwise to 150 mL distilled water under vigorous stirring. The droplet size was reduced by sonication at ambient temperature for 60 min. The emulsion was then stirred at ambient temperature for overnight to evaporate the methylene chloride. The aggregated AM-loaded micelles were removed by centrifugation (3000 rpm × 30 min). The aqueous micelles solution was then dried at room temperature by a vacuum rotary evaporator. The unloaded AM was eliminated by washing three times with distilled water because of the solubility of AM in water is much greater than that of the block copolymer and micelle. The micelles were then obtained by vacuum drying. A weighed amount of micelle was disrupted by the addition of acetonitrile (20 mL). Drug content was assayed spectrophotometrically at 240 nm using a Diode Array UV-vis Spectrophotometer. Equations (1) and (2) calculate the drug-loading content and drug entrapment efficiency of micelle, respectively:

$$\text{Drug} - \text{loading content}\ (\%) = (\text{weight of drug in micelles}/\text{weight of micelles}) \times 100 \quad (1)$$

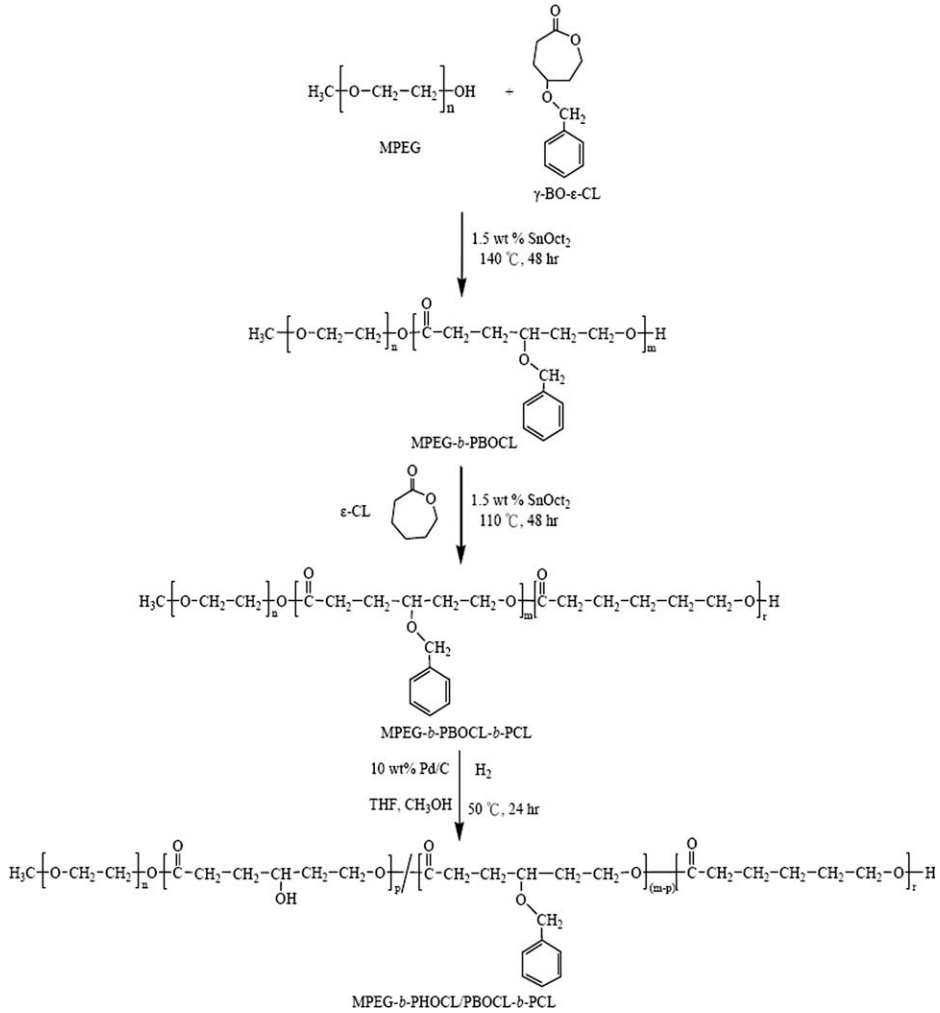

Scheme 1 The synthesis of MPEG-*b*-PHOCL/PBOCL-*b*-PCL block copolymers.

$$\text{Drug entrapment efficiency (\%)} = (\text{weight of drug in micelles} / \text{weight of drug fed initially}) \times 100 \quad (2)$$

In vitro drug release studies

The appropriate amounts of the AM-loaded micelles (110.2 mg) were precisely weighed and suspended in 10 mL of PBS (0.01 M, pH 7.4). the micellar solution was introduced into a dialysis membrane bag (molecular weight cutoff = 3500), and the bag was placed in 50 mL of PBS release media; the media were shaken (30 rpm) at 37°C. At predetermined time intervals, 3 mL aliquots of the aqueous solution were withdrawn from the release media, and the same volume of a fresh buffer solution was added. The concentration of released AM was monitored with a UV-vis spectrophotometer at a wavelength of 240 nm. The rate of controlled drug release was measured by the accumulatively released weight of AM according to the calibration curve of AM.

RESULTS AND DISCUSSION

Synthesis and characterization of $MPEG_{12}$-*b*-PBOCL diblock copolymers

Various $MPEG_{12}$-*b*-PBOCL diblock copolymers were synthesized by the ring-opening polymerization (ROP) of 4-benzyloxy-ε-CL (4-BOCL) with the hydroxyl-terminated macroinitiator $MPEG_{12}$ (M_n = 550 g mol^{-1}). Scheme 1 illustrates the synthesis of the amphiphilic $MPEG_{12}$-*b*-PBOCL block copolymers. The $MPEG_{12}$ hydroxyl group was used as the initiation site for the ROP of 4-BOCL. The influence of the polymerization time on the copolymerization of 4-BOCL and $MPEG_{12}$ (with molar ratio 10/1) was investigated at 140°C in the presence of $SnOct_2$ (1.5 wt %) as a catalyst for various times. Figure 3 depicts the M_n and M_w/M_n of the copolymers. As the polymerization time increased from 12 to 48 h, the M_n of the copolymers increased from 1350 to 2200 g mol^{-1}($M_{n,th}$ = 2750 g mol^{-1}) and M_w/M_n increased from 1.14 to 1.40. With a fixed macroinitiator, copolymers with different compositions were prepared by changing the comonomer 4-BOCL feed

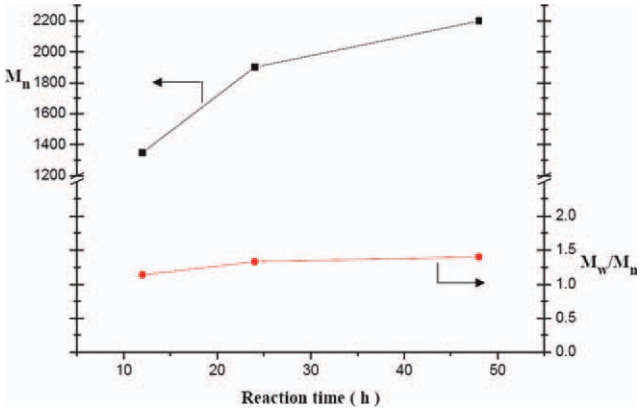

Figure 3 Effect of reaction time on the M_n and M_w/M_n on MPEG-*b*-PBOCL polymer prepared by polymerization of $MPEG_{12}$ and 4-BOCL using 1.5 wt % $SnOct_2$ as a catalyst at 140°C. [Color figure can be viewed in the online issue, which is available at wileyonlinelibrary.com.]

ratio. Table I compiles the polymerization results, showing high yields between 86 and 96%. The 4-benzyloxy substitution of ε-CL reduces the polymerization rate, as also observed for other substituted lactones.[29,30] M_ns of the block copolymers obtained from the copolymerization of 4-BOCL and $MPEG_{12}$ increased with the increase of the molar ratios of 4-BOCL to $MPEG_{12}$ in feed. When the molar ratios of 4-BOCL to $MPEG_{12}$ in feed increased from 10 to 50, the M_ns of the copolymer increased from 2210 to 7320 g mol^{-1} with M_w/M_n between 1.26 and 1.58. The molar ratio of the compositions in the block copolymers was analyzed by ^1H NMR [Fig. 1(A)]. The amounts of comonomer incorporated into the copolymer can be calculated by comparing the integral area of the resonance peaks $\delta = 4.51$ ppm of the methylene protons (H_i) of PBOCL with the resonance peaks $\delta = 3.39$ ppm of the terminal methoxy protons (H_a) in MPEG. The degree of polymerization (DP) calculated by comparing the integral area of the resonance peaks 3 $I_{H_i}/2$ I_{H_a}. According to ^1H NMR spectroscopy, the conversion of copolymerization in the monomers was lower than the corresponding feeds at higher the molar ratios of monomer in feed. This is probably because the substituted lactones polymerize significantly slower than ε-caprolactone, and stems from some transesterification. When the molar ratio of [4-BOCL]/[$MPEG_{12}$] in feed exceeds 50, a maximum limitation for polymerization was observed. This suggests that the conjugative effect and the spatial hindrance of benzyloxy group have a strong influence on polymerization. The resulting polymer showed a broad polydispersity ($M_w/M_n = 1.57$) compared with the unfunctionalized PEO-*b*-PCL ($M_w/M_n = 1.04$) and tailing in its GPC chromatogram [Fig. 4(A)], which may be attributed to the presence of traces of PBOCL homopolymer in the reaction product.

Synthesis and characterization of $MPEG_{12}$-*b*-PBOCL-*b*-PCL block copolymer

According to Scheme 1, a series of functional $MPEG_{12}$-*b*-PBOCL-*b*-PCL triblock copolymers were obtained via the ROP of ε-CL with the hydroxyl-terminated diblock macroinitiator $MPEG_{12}$-*b*-PBOCL. With a fixed amount of $MPEG_{12}$-*b*-PBOCL macroinitiator, copolymers with different compositions were prepared by changing the monomer ε-CL feed ratios for $SnOct_2$-catalyzed polymerization at 110°C for 24 h. Table II compiles these polymerization results, showing that yields were moderate. The M_n values of the obtained triblock copolymers increased with an increase of the molar ratios of ε-CL to $MPEG_{12}$-*b*-PBOCL in feed. When the $MPEG_{12}$-*b*-$PBOCL_{12}$ was used as the macroinitiator, the molar ratios of ε-CL to $MPEG_{12}$-*b*-$PBOCL_{12}$ in feed increased from 30 to 90 and the M_ns of the copolymers increased from 4480 to 7980 g mol^{-1}, with M_w/M_n between 1.49 and 1.66. Similarly, if $MPEG_{12}$-*b*-$PBOCL_{27}$ was used as the macroinitiator, the M_ns of the block copolymers increased with the increase of the molar ratios of ε-CL to $MPEG_{12}$-*b*-$PBOCL_{27}$ in feed. The molar ratios of the compositions in the block copolymers were analyzed with ^1H NMR. The amounts of the

TABLE I
Results of the Block Copolymerization of 4-Benzyloxy-ε-Caprolactone (4-BOCL) Initiated with $MPEG_{12}$ in Bulk at 140°C with 1.5 wt % $SnOct_2$ as the Catalyst for 48 h

Copolymer	[$MPEG_{12}$]/[4-BOCL] molar ratio in feed	[$MPEG_{12}$]/[4-BOCL] molar ratio[a]	$M_{n,NMR}$[a] (g mol^{-1})	$M_{n\ th}$[b] (g mol^{-1})	$M_{n,GPC}$[c] (g mol^{-1})	M_w/M_n[c]	Yield (%)	T_g[d] (°C)
$MPEG_{12}$-*b*-$PBOCL_{12}$	1/10	1/12	3190	2750	2210	1.26	86	−37.5
$MPEG_{12}$-*b*-$PBOCL_{27}$	1/30	1/27	6490	7150	3640	1.57	93	−28.9
$MPEG_{12}$-*b*-$PBOCL_{31}$	1/50	1/31	7370	11,530	7320	1.58	96	–

[a] Determine by ^1H NMR spectroscopy.
[b] $M_{n,th} = M_{n,MPEG} + M_{4\text{-BOCL}} \times$ [4-BOCL]/[$MPEG_{12}$] (where $M_{n,MPEG}$ is the number –average molecular weight of MPEG, $M_{4\text{-BOCL}}$ is the molecular weight of 4-BOCL. [4-BOCL] is the monomer 4-BOCL molarity concentration, and [$MPEG_{12}$] is the initiator MPEG molarity concentration).
[c] Determined by GPC.
[d] Determined from DSC thermograms.

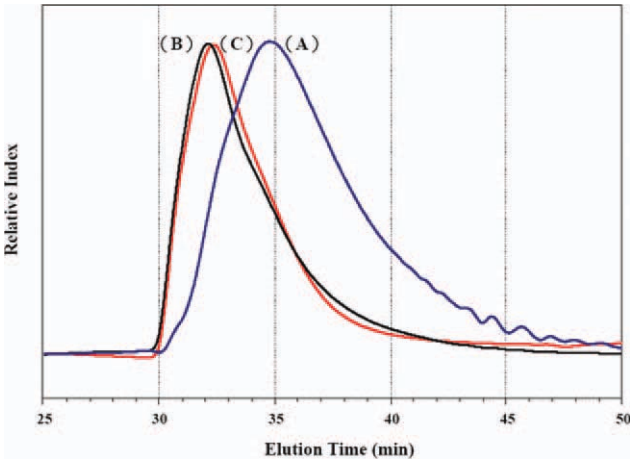

Figure 4 GPC curves of (A) $MPEG_{12}$-*b*-$PBOCL_{27}$, (B) $MPEG_{12}$-*b*-$PBOCL_{27}$-*b*-PCL_{89}, and (C) deprotected $MPEG_{12}$-*b*-$PHOCL_{22}$/$PBOCL_5$-*b*-PCL_{89}. [Color figure can be viewed in the online issue, which is available at wileyonlinelibrary.com.]

monomer incorporated into the copolymer can be calculated by comparing the integral area of the resonance peaks (δ = 3.39 ppm) of the terminal methoxy protons (H_a) of $MPEG_{12}$-*b*-PBOCL with the resonance peaks (δ = 1.64 ppm) of the C_3 and C_5 methylene protons (H_{1+n}) of PCL. The DP calculated by comparing the integral area of the resonance peaks 3 $I_{H1+n}/4\ I_{Ha}$. The copolymerization conversion of the ε-CL was significantly higher than the corresponding feeds because of its high reactivity in the polymerization. Figure 1(B) shows the typical ^{1}H NMR spectrum of triblock copolymer $MPEG_{12}$-*b*-$PBOCL_{27}$-*b*-PCL_{48} with a molar ratio of [ε-CL]/[$MPEG_{12}$-*b*-$PBOCL_{27}$] = 48. The peaks are assigned to the corresponding hydrogen atoms of the copolymers. Figure 4 compares the typical GPC curves of the triblock copolymers with those of the original $MPEG_{12}$-*b*-$PBOCL_{27}$ macroinitiator. The GPC traces show a unimodal distribution of the block copolymer and do not show the presence of any possible homopolymerized PCL. In each block copolymer, the peak [Fig. 4(B)] shifted toward a higher molecular weight region compared with the peak [Fig. 4(A)] of the original $MPEG_{12}$-*b*-$PBOCL_{27}$ macroinitiator, with little change in the molecular weight distribution. These preliminary results show that the block copolymerization of the hydroxyl-group terminated $MPEG_{12}$-*b*-$PBOCL_{27}$ macroinitiator and ε-CL using $SnOct_2$-catalyst was successful under the experimental conditions used.

Deprotection of the benzyl protecting group of the new copolymer

The benzyl protective groups of $MPEG_{12}$-*b*-PBOCL-*b*-PCL can be removed by catalytic-transfer

TABLE II
Results of The Block Copolymerization of ε-Caprolactone (ε-CL) Initiated with $MPEG_{12}$-*b*-PBOCL in Bulk at 110°C with 1.5 wt % $SnOct_2$ as the Catalyst for 24 h

Copolymer	[MPEG-*b*-PBOCL]/[ε-CL] molar ratio in feed	[MPEG-*b*-PBOCL]/[ε-CL] molar ratio[a]	$M_{n,NMR}$[a] (g mol^{-1})	$M_{n,th}$[b] (g mol^{-1})	$M_{n,GPC}$[c] (g mol^{-1})	M_w/M_n[c]	Yield (%)	T_g[d] (°C)	T_m[d] (°C)
$MPEG_{12}$-*b*-$PBOCL_{12}$-*b*-PCL_{33}	1/30	1/33	6950	6170	4480	1.57	63	−45.2	39.4
$MPEG_{12}$-*b*-$PBOCL_{12}$-*b*-PCL_{59}	1/60	1/59	9920	9590	5440	1.49	61	−47.9	48.2, 40.7
$MPEG_{12}$-*b*-$PBOCL_{12}$-*b*-PCL_{146}	1/90	1/146	19,830	13,010	7980	1.66	89	−50.8	54.6, 50.7
$MPEG_{12}$-*b*-$PBOCL_{27}$-*b*-PCL_8	1/10	1/8	7400	8290	4290	1.57	70	−27.9	–
$MPEG_{12}$-*b*-$PBOCL_{27}$-*b*-PCL_{48}	1/30	1/48	11,960	10,370	8270	1.56	87	−43.8	35.6
$MPEG_{12}$-*b*-$PBOCL_{27}$-*b*-PCL_{89}	1/60	1/89	16,640	13,990	9730	1.37	67	−50.6	40.6
$MPEG_{12}$-*b*-$POHCL_{22}$/$PBOCL_5$-*b*-PCL_{89}	1/60	–	14,660	14,210	10,920	1.45	51	−49.1	50.3, 43.3

[a] Determined by ^{1}H NMR spectroscopy of MPEG-*b*-PBOCL-*b*-PCL.
[b] $M_{n,th}$ of MPEG-*b*-PBOCL-*b*-PCL = $M_{n,MPEG\text{-}b\text{-}PBOCL}$ + [ε-CL]/[MPEG-*b*-PBOCL] × $M_{\varepsilon\text{-}CL}$ (where $M_{n,MPEG\text{-}b\text{-}PBOCL}$ is the number-average molecular weight of MPEG-*b*-PBOCL, $M_{\varepsilon\text{-}CL}$ is the molecular weight of ε-CL, [ε-CL] is the monomer ε-CL molarity concentration, and [MPEG-*b*-PBOCL] is the macroinitiator MPEG-*b*-PBOCL molarity concentration).
[c] Determined by GPC.
[d] Determined from DSC thermograms.

hydrogenation. The FT-IR results in Fig. 2(B) confirm the deprotection of $MPEG_{12}$-*b*-$PBOCL_{27}$-*b*-PCL_{89}. Compared with the IR spectrum of the benzyl protected copolymers, the most distinctive features of the deprotected $MPEG_{12}$-*b*-$PBOCL_{27}$-*b*-PCL_{89} are the almost complete absence of aromatic C—H (out-of-plane bending) vibration absorption at 700 and 737 cm^{-1} from the benzyl protected group and the presence of a broad hydroxyl vibration band from 3100 to 3600 cm^{-1}. This indicates the removal of the benzyl group. Figure 4(C) shows the GPC trace of the deprotected polymer. Compared with that of $MPEG_{12}$-*b*-$PBOCL_{27}$-*b*-PCL_{89} [Fig. 4(B)], its peak shifted to the lower molecular weight side due to the removal of the protecting groups, and its M_w/M_n remains unchanged. This implies that the main-chain degradation of the polymer is negligible. A comparison with the ^1H NMR spectrum of the protected copolymer shows that the peaks around δ = 4.50 and 7.32 ppm, which were assigned to the hydrogen atoms of the benzyl protecting group, decreased in the spectrum of the deprotected copolymer after 24 h of hydrogenation. However, the ^1H NMR spectrum data also reveals that about 19% of the benzyl groups remain unremoved. This is mainly due to the higher steric effect of copolymer which might prevent benzyl group from coming into contact with the Pd/C powder. As the reaction time up to 30 h, the M_n decrease dramatically due to the hydrogenolysis.

Thermal properties

Figure 5 shows the thermal behaviors of the block copolymers and DSC curves of $MPEG_{12}$-*b*-PBOCL and $MPEG_{12}$-*b*-PBOCL-*b*-PCL. The DSC curves show that fixing the length of the MPEG block (M_n = 550 g mol^{-1}) and increasing the length of PBOCL block produces an increase in T_gs. The T_gs of MPEG-*b*-PBOCL is higher than that in MPEG-*b*-PCL. This is due to the steric hindrance of 4-BOCL containing the benzyl substituents, which reduces the flexibility of the backbone. Incorporating larger amounts of 4-BOCL into the macromolecular backbone causes a slight increase in T_g. For the $MPEG_{12}$-*b*-PBOCL-*b*-PCL system, an increased amount of ε-CL incorporated into the copolymers caused a decreased in T_g, and an increase in T_ms of the copolymers. The values of T_g, decreased from −45.2 to −50.8°C, while T_ms increased from 39.4 to 54.6°C when the [ε-CL]/[$MPEG_{12}$-*b*-$PBOCL_{12}$] molar ratios increased from 33 to 146. Similarly, T_g decreased and T_ms increased in the copolymers when the [ε-CL]/[$MPEG_{12}$-*b*-$PBOCL_{27}$] molar ratios increased from 8 to 89. This is due to the fact that the copolymers have a higher molecular weight when larger amounts of ε-CL are incorporated into the macromolecular backbone,

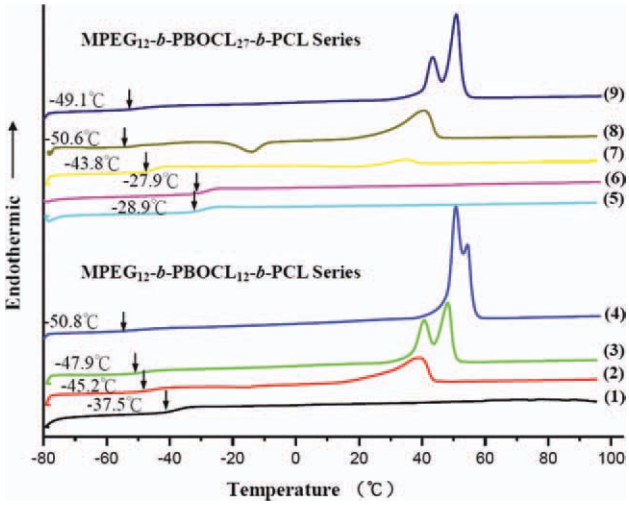

Figure 5 DSC curves of (1) $MPEG_{12}$-*b*-$PBOCL_{12}$, (2) $MPEG_{12}$-*b*-$PBOCL_{12}$-*b*-PCL_{33}, (3) $MPEG_{12}$-*b*-$PBOCL_{12}$-*b*-PCL_{59}, (4) $MPEG_{12}$-*b*-$PBOCL_{12}$-*b*-PCL_{146}, (5) $MPEG_{12}$-*b*-$PBOCL_{27}$, (6) $MPEG_{12}$-*b*-$PBOCL_{27}$-*b*-PCL_8, (7) $MPEG_{12}$-*b*-$PBOCL_{27}$-*b*-PCL_{48}, (8) $MPEG_{12}$-*b*-$PBOCL_{27}$-*b*-PCL_{89}, (9) deprotected $MPEG_{12}$-*b*-$PHOCL_{22}$/$PBOCL_5$-*b*-PCL_{89}. [Color figure can be viewed in the online issue, which is available at wileyonlinelibrary.com.]

causing a decrease in T_g, and an increased in T_ms. The existence of two melting temperature very close together might be the primary and secondary crystallization of PCL. However, the T_m of the copolymers was slightly lower than that of the PCL (T_m = 58.3°C),[31] indicating that the presence of $MPEG_{12}$-*b*-PBOCL blocks decreases the crystallinity of the copolymer with respect to the PCL homopolymer by reducing the PCL chain mobility. The crystallinity of PCL is suppressed when its molecular weight is too low for $MPEG_{12}$-*b*-$PBOCL_{27}$-*b*-PCL_8.

Micelles of block copolymers

The amphiphilic nature of the block copolymers, consisting of hydrophilic MPEG, and hydrophobic PBOCL as well as PCL blocks, provides an opportunity to form micelles in water. The characteristics of the block copolymer micelles in an aqueous phase were investigated by fluorescence techniques. The critical micelle concentrations (CMCs) values of the block copolymers in an aqueous phase were determined by a fluorescence technique using pyrene as a probe.

Figure 6 shows the excitation spectra of pyrene in $MPEG_{12}$-*b*-$PBOCL_{12}$-*b*-PCL_{33} solutions with various concentrations. As it can be seen, the fluorescence intensity increases with the increase in the concentration of $MPEG_{12}$-*b*-$PBOCL_{12}$-*b*-PCL_{33}. The characteristic feature of pyrene excitation spectra, a red shift of the (0, 0) band from 334 to 338 nm upon pyrene partition into micellar hydrophobic core, was

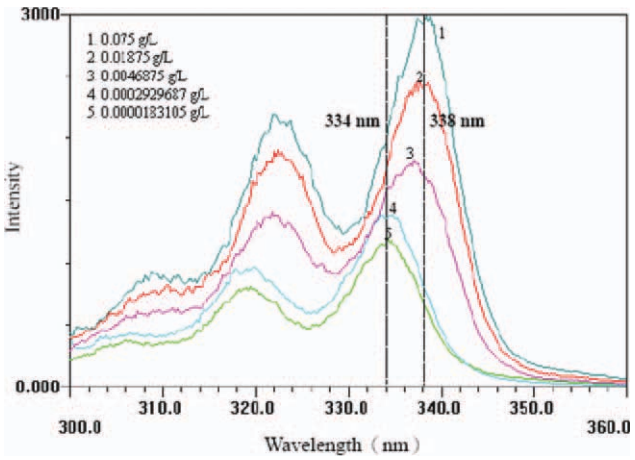

Figure 6 Excitation spectra of pyrene as a function of $MPEG_{12}$-*b*-$PBOCL_{12}$-*b*-PCL_{33} concentration in deionized water (λ_{em} = 390 nm). [Color figure can be viewed in the online issue, which is available at wileyonlinelibrary.com.]

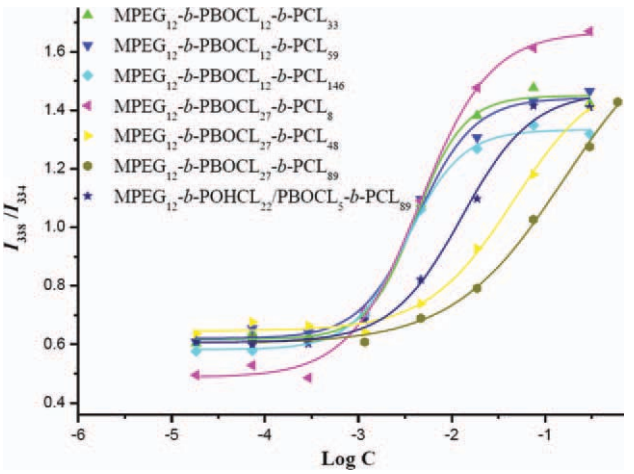

Figure 7 Plot of the I_{338}/I_{334} intensity ratio (from pyrene excitation spectra; pyrene concentration = $6.1 \times 10^{-7}M$) versus the logarithm of the concentration (log *C*) for MPEG-*b*-PBOCL-*b*-PCL and deprotecting MPEG-*b*-PBOCL-*b*-PCL triblock copolymers (λ_{em} = 390 nm). [Color figure can be viewed in the online issue, which is available at wileyonlinelibrary.com.]

utilized to determine the CMC values of $MPEG_{12}$-*b*-PBOCL, and $MPEG_{12}$-*b*-PBOCL-*b*-PCL block copolymers. Figure 7 shows the intensity ratios (I_{338}/I_{334}) of pyrene excitation spectra versus the logarithm of $MPEG_{12}$-*b*-PBOCL-*b*-PCL, and deprotected $MPEG_{12}$-*b*-$PHOCL_{22}$/$PBOCL_5$-*b*-PCL_{89} block copolymers' concentration. As the polymer concentration reached a certain concentration (i.e., the CMC), the value of I_{338}/I_{334} increased dramatically in a sigmoid manner. The CMC was determined from the intersection of straight line segments, drawn through the points at the lowest polymer concentrations, which lie on a nearly horizontal line, with that going through the points on the rapidly rising part of the plot. Table III shows the CMC values of the block copolymers depending on the block composition. At the fixed length of the hydrophilic block, the CMC values decreased from 1.74 to 1.07 mg L^{-1} for $MPEG_{12}$-*b*-PBOCL, and from 1.29 to 0.80 mg L^{-1} for $MPEG_{12}$-*b*-$PBOCL_{12}$-*b*-PCL_{33-146}, respectively, with increasing of hydrophobic PBOCL and/or PCL chain length. The lower CMC values for MPEG-*b*-PBOCL based-block polymers clearly show that introducing hydrophobic benzyloxy groups to the poly(ε-caprolactone) encourages the self-association of block copolymers. In contrast, the CMC values of the block copolymers increased from 0.76 to 9.77 mg L^{-1} for $MPEG_{12}$-*b*-$PBOCL_{27}$-*b*-PCL_{8-89}, as the hydrophobic PCL chain length increased. Until now, we did not know the reason clearly. A probable reason is that the micellization ability reduces with increasing length of the hydrophobic PCL segment. More importantly, the presence of an aromatic group on the PCL block seems to be even more effective than elongating the PCL block in pushing the CMC to lower

TABLE III
Properties of Copolymer Micelles

Copolymer	CMC[a] (mg L^{-1})	Unloaded AM micelle			AM-loaded micelle	
		Size[b] (nm)	PDI	Zeta potential[b] (mv)	Size[b] (nm)	PDI
$MPEG_{12}$-*b*-$PBOCL_{12}$	1.74	155.9 ± 3.1	0.12 ± 0.02	−16.8 ± 0.8	134.8 ± 1.3	0.12 ± 0.01
$MPEG_{12}$-*b*-$PBOCL_{27}$	1.07	145.1 ± 1.8	0.04 ± 0.02	−20.7 ± 1.0	120.7 ± 0.3	0.17 ± 0.01
$MPEG_{12}$-*b*-$PBOCL_{12}$-*b*-PCL_{33}	1.29	175.1 ± 1.1	0.07 ± 0.02	−12.5 ± 0.8	120.1 ± 1.0	0.14 ± 0.01
$MPEG_{12}$-*b*-$PBOCL_{12}$-*b*-PCL_{59}	0.95	143.8 ± 0.1	0.17 ± 0.01	−5.8 ± 0.3	89.4 ± 0.5	0.12 ± 0.01
$MPEG_{12}$-*b*-$PBOCL_{12}$-*b*-PCL_{146}	0.80	134.4 ± 4.6	0.26 ± 0.03	−2.6 ± 0.2	90.3 ± 2.6	0.11 ± 0.02
$MPEG_{12}$-*b*-$PBOCL_{27}$-*b*-PCL_8	0.76	168.5 ± 0.3	0.04 ± 0.01	−9.8 ± 0.2	105.2 ± 0.9	0.11 ± 0.01
$MPEG_{12}$-*b*-$PBOCL_{27}$-*b*-PCL_{48}	5.01	119.8 ± 2.7	0.16 ± 0.02	−4.5 ± 0.4	102.3 ± 0.7	0.10 ± 0.01
$MPEG_{12}$-*b*-$PBOCL_{27}$-*b*-PCL_{89}	9.77	87.0 ± 0.7	0.12 ± 0.01	−2.3 ± 0.1	97.8 ± 2.2	0.29 ± 0.01
$MPEG_{12}$-*b*-$PHOCL_{22}$/ $PBOCL_5$-*b*-PCL_{89}	2.14	193.2 ± 6.4	0.25 ± 0.06	−5.7 ± 0.5	–	–

[a] Determined by fluorescence.
[b] Determined by DLS.

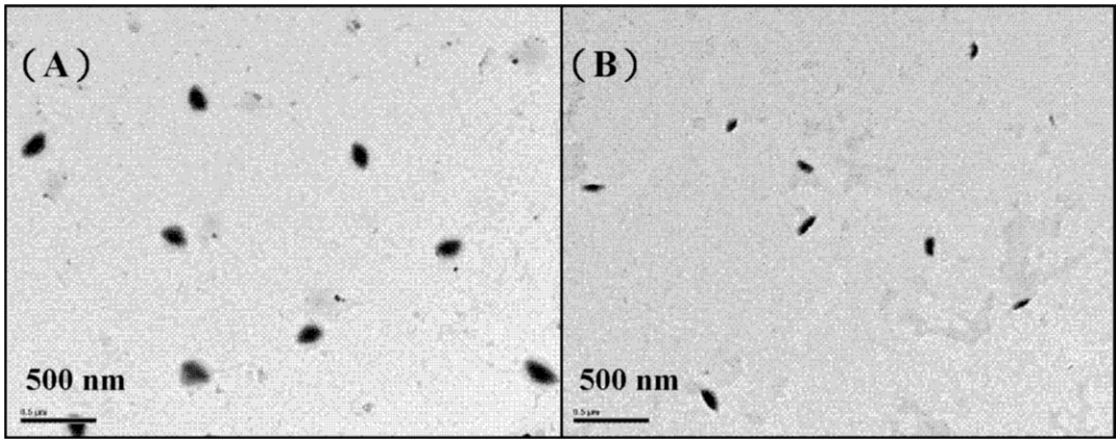

Figure 8 TEM photograph of the micelles formed by (A) $MPEG_{12}$-*b*-$PBOCL_{12}$-*b*-PCL_{59} and (B) AM-loaded $MPEG_{12}$-*b*-$PBOCL_{12}$-*b*-PCL_{59}.

concentrations. However, note that the rigidity of the micellar core over a limit, the micelle was converted into less stable. When the $MPEG_{12}$-*b*-$PBOCL_{27}$-*b*-PCL_{89} was deprotected, the CMC values of the copolymer decreased from 9.77 to 2.14 mg L^{-1}. This demonstrated that hydrophilicity increases when the protecting groups of PBOCL are deprotected.

The mean hydrodynamic diameters of micelles from DLS ranged from 87 to 200 nm, showing a monodisperse unimodel size distribution pattern. These results indicate that the micelles size depends on the polymer composition. Fixing the concentration of micelle at 50-fold CMC (50 × CMC) value, the size of micelles decreases as the ratio of hydrophobic segment to the hydrophilic segment in copolymer increases. The micellar population showed a small distribution (PDI = 0.04–0.29) for unloaded and loaded AM micelles. In contrast to the micelle size of the deprotected $MPEG_{12}$-*b*-$PHOCL_{22}$/$PBOCL_5$-*b*-PCL_{89} was bigger than that of the protected $MPEG_{12}$-*b*-$PBOCL_{27}$-*b*-PCL_{89}. This may be attributed to the enhancement of dipole-dipole repulsion of hydroxyl groups or the enlargement of hydrated diameter after deprotecting. Comparing the sizes of loaded and unloaded AM drug micelles shows that the size decreases when AM in loaded in $MPEG_{12}$-*b*-PBOCL-*b*-PCL micelles. This is attributed to the AM-loaded reduce the hydrophobic/hydrophobic repulsion of PCL that result the constringency of core. Figure 8 shows the morphology of the micelles formed by $MPEG_{12}$-*b*-PBOCL-*b*-PCL. Amphiphilic block copolymers with the length of the core-forming block much greater than the corona-forming block form crew cut aggregates have been shown to produce a wide range of morphologies.[32] These images confirm that the copolymers formed almost nanoparticle with spindle shapes due to the degree of stretching of the core-forming block too larger to support the spherical morphology, at which form the spindle morphology.[33]

Zeta potential, i.e., the surface charge, greatly influences particle stability in suspension through the electrostatic repulsion between particles. The general dividing line between stable and unstable suspensions is generally taken at either +30 mV or −30 mV. The zeta potential in the range −20.7 mV to −2.3 mV demonstrated the resulting micelles are instable to moderate stable. When the length of PCL increased, the zeta potential reduced rapidly. This may be due to the less electron density PCL segment was incorporated into the backbone.

Drug-loading content and drug entrapment efficiency

The antidepressant drug AM was selected as a model drug. Table IV summarizes the drug-loading content and drug entrapment efficiency of MPEG-*b*-PBOCL, $MPEG_{12}$-*b*-PBOCL-*b*-PCL and deprotected $MPEG_{12}$-*b*-PHOCL-*b*-PCL block copolymeric micelles. The drug-loading content and drug entrapment efficiency depends mainly on the composition of the copolymer and the AM to polymer feed weight ratio. For protected $MPEG_{12}$-*b*-$PBOCL_{12}$-*b*-PCL_{33}, as the feed weight ratio of AM to polymer increased from 0.1 to 1, the drug entrapment efficiency increased from 2.4 to 4.1%. For protected $MPEG_{12}$-*b*-$PBOCL_{12}$-*b*-PCL_{33}, the drug-loading content increased with an increasing weight ratio of drug to polymer. The reason for this is rather complicated, and can be affected by many factors, such as molecular weight, the ratio of hydrophobic segment to hydrophilic segment, crystallinity, and so on.[34] For an AM to polymer feed weight ratio fixed at 1, the drug entrapment efficiency and the drug-loading content increased as the length of hydrophobic segment increased. The drug entrapment efficiency of the $MPEG_{12}$-*b*-$PBOCL_{27}$-*b*-

TABLE IV
Drug Entrapment Efficiency and Drug Loading of AM-Loaded Copolymer Micelles

Copolymer	Feed weight ratio (AM/polymer)	Drug entrapment efficiency (%)	Drug loading (%)
$MPEG_{12}$-*b*-$PBOCL_{12}$	1/1	1.72 ± 0.03	0.86 ± 0.01
$MPEG_{12}$-*b*-$PBOCL_{27}$	1/1	5.34 ± 0.08	2.67 ± 0.04
$MPEG_{12}$-*b*-$PBOCL_{12}$-*b*-PCL_{33}	1/10	2.41 ± 0.09	0.21 ± 0.01
	1/4	2.48 ± 0.35	0.49 ± 0.07
	1/2	3.88 ± 0.14	1.28 ± 0.05
	1/1	4.13 ± 0.24	2.07 ± 0.12
$MPEG_{12}$-*b*-$PBOCL_{12}$-*b*-PCL_{59}	1/1	10.06 ± 0.43	5.03 ± 0.21
$MPEG_{12}$-*b*-$PBOCL_{12}$-*b*-PCL_{146}	1/1	1.59 ± 0.15	0.80 ± 0.08
$MPEG_{12}$-*b*-$PBOCL_{27}$-*b*-PCL_{8}	1/1	1.35 ± 0.21	0.68 ± 0.11
$MPEG_{12}$-*b*-$PBOCL_{27}$-*b*-PCL_{48}	1/1	4.87 ± 0.04	2.43 ± 0.02
$MPEG_{12}$-*b*-$PBOCL_{27}$-*b*-PCL_{89}	1/1	17.03 ± 0.90	8.52 ± 0.46
$MPEG_{12}$-*b*-$PHOCL_{22}$/$PBOCL_5$-*b*-PCL_{89}	1/1	2.46 ± 0.03	1.23 ± 0.01

PCL_{48} is significantly lower than the $MPEG_{45}$-*b*-PCL_{45}.[25] This due to have more steric hindrance hydrophobic segment in $MPEG_{12}$-*b*-$PBOCL_{27}$-*b*-PCL_{48} block copolymers, hinder the less amount of drug entrapped in micelles.

Preliminary *in vitro* drug release study

The antidepressant drug AM was selected as a model drug to investigate the controlled drug release property of the $MPEG_{12}$-*b*-$PBOCL_{27}$-*b*-PCL_{89} and deprotected $MPEG_{12}$-*b*-$PHOCL_{22}$/$PBOCL_5$-*b*-PCL_{89} micelles *in vitro*. The release rate was monitored by the determination of the concentration of the accumulatively released drug. Release profiles of AM from the $MPEG_{12}$-*b*-$PBOCL_{27}$-*b*-PCL_{89} and deprotected $MPEG_{12}$-*b*-$PHOCL_{22}$/$PBOCL_5$-*b*-PCL_{89} micelles are shown in Figure 9. The cumulative release of AM was around 95% within 8 h. Two phases of release can be distinguished: an initial drug burst, where AM located close to the surface of microparticles is released and secondly a phase in which AM is released, probably by passive pore-diffusion mechanism. The initial release amount (burst release) of AM from the micelles of deprotected $MPEG_{12}$-*b*-$PHOCL_{22}$/$PBOCL_5$-*b*-PCL_{89} was slight lower compared with that from the micelles of $MPEG_{12}$-*b*-$PBOCL_{27}$-*b*-PCL_{89}. This is due to the strong interaction of AM with the deprotected $MPEG_{12}$-*b*-$PHOCL_{22}$/$PBOCL_5$-*b*-PCL_{89}.

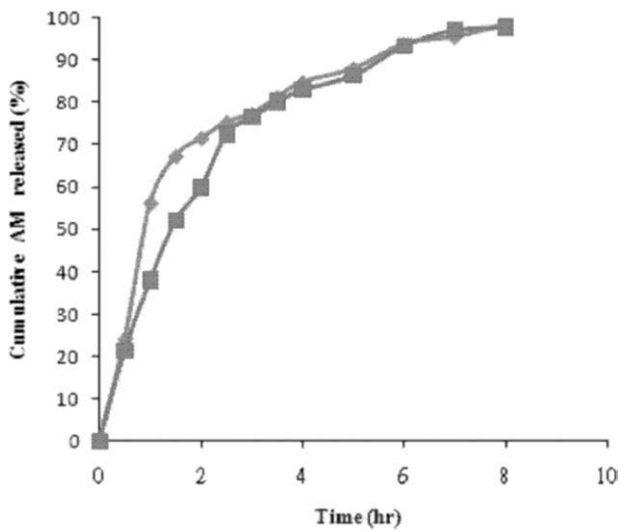

Figure 9 AM release profiles of (◆) the $MPEG_{12}$-*b*-$PBOCL_{27}$-*b*-PCL_{89} and (■) the deprotected $MPEG_{12}$-*b*-$PHOCL_{22}$/$PBOCL_5$-*b*-PCL_{89} micelles in PBS solution at 37°C.

CONCLUSIONS

A series of novel MPEG-*b*-PCL based-block copolymers with functional 4-benzyloxy or hydroxyl groups was synthesized through the successful ROP of MPEG with 4-BOCL and ε-CL. The resulting MPEG-*b*-PBOCL diblock copolymers were amorphous, exhibited only T_g. Incorporating larger amounts of 4-BOCL into the macromolecular backbone caused a slight increase in T_g. However, incorporating an increased amount of ε-CL into the copolymers caused a decrease in T_g and an increase in T_ms in the triblock copolymers. These functional copolymers can easily form micelles in aqueous solution. The amphiphilic nature of the block copolymer can be tuned by the chain lengths of PBOCL/PCL block segments. The mean hydrodynamic diameter of the micelles ranges from 87 to 200 nm, and they exhibit a spindle shape. The drug-loading content and drug entrapment efficiency of these micelles depends mainly on the composition of the copolymer and the AM to polymer feed weight ratio.

References

1. Kataoka, K.; Harada, A.; Nagasaki, Y. Drug Deliv Rev 2001, 47, 113.

2. Lavasanifar, A.; Samuel, J.; Kwon, G. S. Adv Drug Deliv Rev 2002, 54, 169.
3. Liggins, R. T.; Burt, H. M. Adv Drug Deliv Rev 2002, 54, 191.
4. Bae, Y.; Fukushima, S.; Harada, A.; Kataoka, K. Angew Chem Int Ed Engl 2003, 42, 4640.
5. Riess, G. Prog Polym Sci 2003, 28, 1107.
6. Miyata, K.; Christie, R. J.; Kataoka, K. React Funct Polym 2011, 71, 227.
7. Chen, S.; Cheng, S. X.; Zhuo, R. X. Macromol Biosci 2011, 11, 576.
8. Nakanishi, T.; Fukushima, S.; Okamoto, K.; Suzuki, M.; Matsumura, Y.; Yokoyama, M.; Okano, T.; Sakurai, Y.; Kataoka, K. J Control Release 2001, 74, 295.
9. Yokoyama, M.; Fukushima, S.; Uehara, R.; Okamoto, K.; Kataoka, K.; Sakurai, Y.; Okano, T. J Control Release 1998, 50, 79.
10. Lavasanifar, A.; Samuel, J.; Sattari, S.; Kwon, G. S. Pharm Res 2002, 19, 418.
11. Li, Y.; Kwon, G. S. Pharm Res 2000, 17, 607.
12. Nishiyama, N.; Kato, Y.; Sugiyama, Y.; Kataoka, K. Pharm Res 2001, 18, 1035.
13. Yokoyama, M.; Satoh, A.; Sakurai, T.; Okano, T.; Matsumura, Y.; Kakizoe, T.; Kataoka, K. J Control Release 1998, 55, 219.
14. Aliabadi, H. M.; Brocks, D. R.; Lavasanifar, A. Biomaterials 2005, 26, 7251.
15. Aliabadi, H. M.; Mahmud, A.; Sharifabadi, A. D.; Lavasanifar, A. J Control Release 2005, 104, 301.
16. Allen, C.; Eisenberg, A.; Mrsic, J.; Maysinger, D. Drug Deliv 2000, 7, 139.
17. Allen, C.; Han, J. N.; Yu, Y. S.; Maysinger, D.; Eisenberg, A. J Control Release 2000, 63, 275.
18. Allen, C.; Yu, Y. S.; Maysinger, D.; Eisenberg, A. Bioconjugate Chem 1998, 9, 564.
19. Forrest, M. L.; Won, C. Y.; Malick, A. W.; Kwon, G. S. J Control Release 2006, 110, 370.
20. Kim, S. Y.; Lee, Y. M. Biomaterials 2001, 22, 1697.
21. Kim, S. Y.; Lee, Y. M.; Shim, H. J.; Kang, J. S. Biomaterials 2001, 22, 2049.
22. Shi, B.; Fang, C.; You, M. X.; Zhang, Y.; Fu, S. K.; Pei, Y. Y. Colloid Polym Sci 2005, 283, 954.
23. Garg, S. M.; Xiong, X. B.; Lu, C.; Lavasanifar, A. Macromolecules 2011, 44, 2058.
24. Mahmud, A.; Xiong, X. B.; Lavasanifar, A. Macromloecules 2006, 39, 9419.
25. Lee, R. S.; Hung, C. B. Polymer 2007, 48, 2605.
26. Trollsås, M.; Lee, V. Y.; Mecerreyes, D.; Löwenhielm, P.; Möller, M.; Miller, R. D.; Hedrick, J. H. Macromolecules 2000, 33, 4619.
27. Wilhelm, M.; Zhao, C. L.; Wang, Y.; Xu, R.; Winnik, A. Macromolecules 1991, 24, 1033.
28. Provencher, S. W.; Hendrix, J. J Chem Phys 1978, 69, 4273.
29. Mecerreyes, D.; Miller, R. D.; Hedrick, J. L.; Detrembleur, C.; Jérôme, R. J Polym Sci Part A: Polym Chem 2000, 38, 870.
30. Parrish, B.; Quansah, J. K.; Emrick, E. J Polym Sci Part A: Polym Chem 2002, 40, 1983.
31. Zhou, J.; Takasu, A.; Ihai, Y.; Hirabayashi, T. Polym J 2004, 36, 182.
32. Yu, K.; Eisenberg, A. Macromolecules 1998, 31, 3509.
33. Christine, A.; Dusica, M.; Adi, E. Colloids Surf B 1999, 16, 3.
34. Hu, Y.; Jiang, X.; Ding, Y.; Zhang, L.; Yang, C.; Zhang, J.; Chen, J.; Yang, Y. Biomaterials 2003, 24, 2395.